

Ostracode Mg/Ca paleothermometry in the North Atlantic and Arctic oceans: Evaluation of a carbonate ion effect

Jesse R. Farmer,^{1,2} Thomas M. Cronin,¹ and Gary S. Dwyer³

Received 22 February 2012; revised 3 May 2012; accepted 5 May 2012; published 21 June 2012.

[1] The reconstruction of deep-sea bottom water temperature (BWT) is important to assess the ocean's response to and role in orbital- and millennial-scale climate change. Deep-sea paleothermometry employs magnesium to calcium (Mg/Ca) ratios in calcitic benthic microfaunas (foraminifera, ostracodes) as a primary proxy method. Mg/Ca paleothermometry may, however, be complicated by bottom water carbonate ion chemistry, which might affect Mg/Ca ratios in shells. To address temperature and carbonate ion influence on Mg/Ca ratios, we studied Mg/Ca ratios in the benthic ostracode genus *Krithe* in the North Atlantic and Arctic oceans using a 686-specimen core top collection, including 412 previously unpublished analyses. Mg/Ca ratios are positively correlated to temperature in multiple species from the North Atlantic [BWT = $(0.885 \times \text{Mg/Ca}) - 5.69$, $r^2 = 0.73$] and for *K. glacialis* in the Arctic Ocean and Nordic Seas [BWT = $(0.439 \times \text{Mg/Ca}) - 5.14$, $r^2 = 0.50$], consistent with previously published calibrations. We found no evidence for a relationship between *Krithe* Mg/Ca and carbonate ion saturation in the North Atlantic Ocean, Nordic Seas, and Arctic Ocean, supporting the use of *Krithe* Mg/Ca for reconstructing past BWT.

Citation: Farmer, J. R., T. M. Cronin, and G. S. Dwyer (2012), Ostracode Mg/Ca paleothermometry in the North Atlantic and Arctic oceans: Evaluation of a carbonate ion effect, *Paleoceanography*, 27, PA2212, doi:10.1029/2012PA002305.

1. Introduction

[2] Reconstructing past changes in deep ocean bottom water temperature (BWT) is important for understanding ocean heat storage and transport, Atlantic meridional overturning circulation, ocean carbon uptake and release during periods of climatic change, and major Cenozoic climate changes. BWT reconstruction using the ratio of magnesium to calcium (Mg/Ca) in the shells of calcitic marine microfossils (benthic foraminifera [Rosenthal *et al.*, 1997]; ostracodes [Corrège, 1993; Dwyer *et al.*, 1995]) has received considerable attention due to the demonstrated temperature dependence of magnesium partitioning in inorganic and biogenic calcite [Chave, 1954; Morse and Mackenzie, 1990] and the proposed insensitivity of Mg/Ca ratios to salinity and ice volume [Rosenthal *et al.*, 1997].

[3] Deepwater temperature reconstructions using benthic foraminiferal Mg/Ca are complicated by several factors. Over Cenozoic timescales, Mg/Ca ratios reflect long-term changes in ocean Mg concentrations as well as temperature

[Lear *et al.*, 2000; Lear, 2007; Coggon *et al.*, 2010; Broecker and Yu, 2011; Bohaty *et al.*, 2012], but changing Mg concentrations probably do not affect reconstructions for the last few million years. Inter-specific differences and physiological overprints during biomineralization (“vital effects”) have been recognized and require independent calibrations for individual taxa [e.g., Bryan and Marchitto, 2008]. Benthic habitat (epifaunal versus infaunal) can influence the degree of exposure to potentially corrosive, carbonate unsaturated bottom water, which can lead to a reduction Mg partitioning coefficients [Elderfield *et al.*, 2006; Rosenthal *et al.*, 2006; Elderfield *et al.*, 2010]. Opinions vary about the degree to which carbonate ion saturation ($\Delta[\text{CO}_3^{2-}] = [\text{CO}_3^{2-}]_{\text{measured}} - [\text{CO}_3^{2-}]_{\text{saturation}}$) influences Mg/Ca in benthic foraminifera, ranging from 30 to 40% of the glacial to interglacial Mg/Ca signal during the Quaternary [Sosdian and Rosenthal, 2009, 2010] to the dominant effect [Yu and Elderfield, 2008; Yu and Broecker, 2010]. As a consequence, although several benthic foraminiferal Mg/Ca-temperature calibrations are now available for shallow and mid-depth species [Kristjánsdóttir *et al.*, 2007; Bamberg *et al.*, 2010; Rosenthal *et al.*, 2011], there remains uncertainty surrounding Mg/Ca-based deepwater temperature reconstructions.

[4] Ostracodes are benthic crustaceans that grow their calcitic shells by molting and have higher Mg concentrations (Mg/Ca ratios ~ 5 to 50 mmol/mol) than foraminiferal tests. Controls on ostracode shell chemistry are relatively well constrained from culturing and field studies of nonmarine and shallow and deep marine ostracode species under known temperature conditions [e.g., Chivas *et al.*, 1986, 1993; De

¹U.S. Geological Survey, Reston, Virginia, USA.

²Now at Lamont-Doherty Earth Observatory, Columbia University, Palisades, New York, USA.

³Division of Earth and Ocean Sciences, Nicholas School of the Environment, Duke University, Durham, North Carolina, USA.

Corresponding author: J. R. Farmer, Lamont-Doherty Earth Observatory, Columbia University, 61 Rte. 9W, PO Box 1000, Palisades, NY 10465, USA. (jfarmer@ldeo.columbia.edu)

©2012. American Geophysical Union. All Rights Reserved.
0883-8305/12/2012PA002305

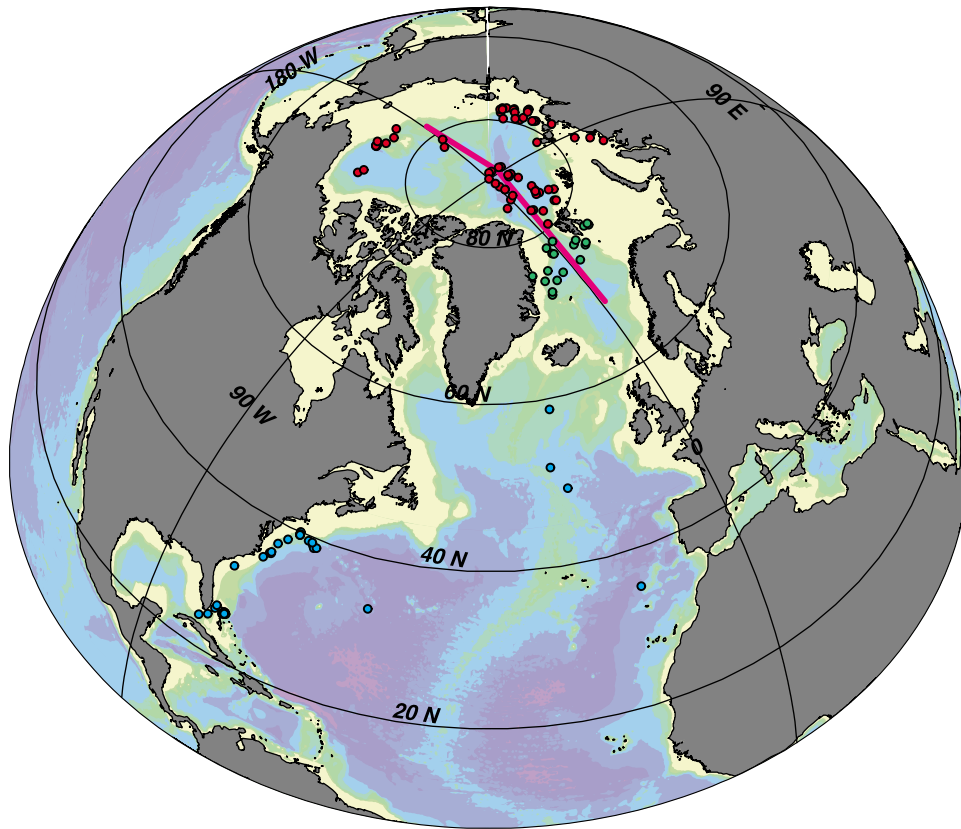


Figure 1. Locations of sites sampled for core top *Krithe* from the northwest Atlantic Ocean (blue circles), Nordic Seas (green circles), and Arctic Ocean (red circles). The path of the transect in Figure 4 is given by the magenta line along the 0° meridian.

Deckker et al., 1999; Holmes and Chivas, 2002; Dwyer et al., 2002; Cronin et al., 2005a]. Mg/Ca ratios in the shells of the ostracode genus *Krithe* have been calibrated to bottom water temperature (BWT) for the North Atlantic [Dwyer et al., 1995] and Arctic oceans [Cronin et al., 1996], and applied to Pliocene and late Quaternary deep-sea BWT reconstruction over orbital [Dwyer et al., 1995; Cronin et al., 2005b; Dwyer and Chandler, 2009] and millennial time-scales [Corrège and De Deckker, 1997; Cronin et al., 1996, 2000; Dwyer et al., 2000]. *Krithe* is an ideal candidate for deep-water temperature reconstructions due to its established taxonomy [Coles et al., 1994], cosmopolitan distribution in deep-sea sediments, and long stratigraphic range (Cretaceous-Recent).

[5] Despite the promise of *Krithe* Mg/Ca-paleothermometry, uncertainty remains in the use of this method due to relatively high Mg/Ca values from the species *K. glacialis* from below 1000 m in the Arctic Ocean and Nordic Seas, and variability in core top calibrations, suggesting that factors other than temperature may exert control on *Krithe* Mg/Ca [Cronin et al., 1996; Dwyer et al., 2002]. Low-temperature variability in epifaunal benthic foraminiferal Mg/Ca ratios has been attributed to the influence of carbonate ion saturation [Elderfield et al., 2006], but the potential for a carbonate ion effect on *Krithe* Mg/Ca in the North Atlantic, Arctic Ocean and Nordic Seas has not been investigated thoroughly. Here we expand the Mg/Ca-temperature calibration data sets of Dwyer et al. [1995] and Cronin et al.

[1996] using new core top *Krithe* specimens from the North Atlantic Ocean, the Nordic Seas (Norwegian, Greenland, Iceland Seas) and the Arctic Ocean, and test the hypotheses that interspecific variability and/or carbonate ion saturation exert a primary control on *Krithe* Mg/Ca.

2. Materials and Methods

[6] Mg/Ca and Sr/Ca ratios from 686 specimens representing eight species of *Krithe* were used in this study, covering a BWT range between -1.7 and 16°C . *Krithe* specimens were obtained from 74 sites in the North Atlantic and 114 sites from the Arctic Ocean and Nordic Seas (Figure 1). Specimens came from multiple cruises and a variety of sampling methods, including box and multicores, core tops of piston cores and Van Veen grabs. To augment core top material obtained from various repositories, R/V *Oceanus* cruise 461 was conducted along the continental slope off the northeastern United States in May 2010, and *Krithe* specimens were retrieved from boxcores covering a range of temperatures (3 to 10°C). We consider samples from the upper 1–2 cm of box and multicores to be the best material for developing a core top calibration, but acknowledge that even these samples may represent time-averaging of 1–2 millennia in low-sedimentation areas.

[7] Sediment samples were soaked and washed over a $63\ \mu\text{m}$ sieve in distilled water, then dried at 50°C in a convection oven. Adult *Krithe* carapaces or valves were

brush-picked from the $>150\ \mu\text{m}$ dry fraction under a binocular light microscope. Species identification in *Krithe* is based on the size and shape of the valve, the distribution of antero-dorsal radial pore canals, and the size and the shape of the inner lamella in adult specimens [Coles *et al.*, 1994]. Each valve or carapace was assigned a preservation index ranging from 1 (transparent) to 7 (opaque white) [Dwyer *et al.*, 1995], and soaked in $\sim 5\%$ NaOCl for 16–24 h to oxidize any remaining organic matter and assist in removal of any adhering particles. Bleach was used as an oxidizing agent due to its efficacy at removal of organic material and its lack of effect on calcite Mg/Ca ratios in preliminary studies [Dwyer *et al.*, 2002]. Each shell was then triple-rinsed in deionized water, visually inspected under light microscope for the presence of any remaining adhering particles, and then twice more rinsed with deionized water under light sonication. Shells were dissolved in 0.05 N nitric acid and the resulting aqueous solution analyzed for Mg, Sr and Ca on a Fisons Instruments Spectraspan 7 DC plasma atomic emission spectrometer (DCP) at Duke University using ultra-pure plasma-grade standard solutions. Analytical precision is approximately 2% based on replicate analysis of samples and standards.

[8] Bottom water temperatures and salinities for each site were estimated from World Ocean Atlas 2001 1/4° grid [Stephens *et al.*, 2002; Boyer *et al.*, 2002] in Ocean Data View (<http://odv.awi.de>). Detailed procedures for calculating $\Delta[\text{CO}_3^{2-}]$ are given in the Appendix. Briefly, $\Delta[\text{CO}_3^{2-}]$ values were calculated using CO2sys (<http://cdiac.ornl.gov/oceans/co2rprt.html>, Lewis and Wallace [1998]) following standard procedures [Yu and Elderfield, 2007; Yu and Elderfield, 2008; Bryan and Marchitto, 2008]. Equilibrium constants K1 and K2 were from Mehrbach *et al.* [1973] refit by Dickson and Millero [1987], with KHSO_4 from Dickson [1990]. We used total alkalinity and total dissolved inorganic carbon (DIC) measurements from locations proximal to our samples in the CARINA [Key *et al.*, 2010] and GLODAP [Key *et al.*, 2004] data sets. Estimates of total phosphate and total silica were from World Ocean Atlas 2009 hydrographic data [Garcia *et al.*, 2010].

[9] DIC concentrations for Atlantic samples were corrected for anthropogenic carbon using anthropogenic DIC estimates from the ΔC^* method [Sabine *et al.*, 2004] available in the GLODAP data set. ΔC^* -derived estimates of anthropogenic DIC are unavailable for the Nordic Seas and Arctic Ocean, so Nordic and Arctic DIC values were corrected for anthropogenic DIC concentrations estimated using the transit time distribution method [Vázquez-Rodríguez *et al.*, 2009; Tanhua *et al.*, 2009]. Preanthropogenic $\Delta[\text{CO}_3^{2-}]$ values converge with modern $\Delta[\text{CO}_3^{2-}]$ values by 3000 m in the North Atlantic and 2000 m in the Nordic Seas and Arctic Ocean (see Figure S1 in the auxiliary material), so DIC concentrations were not corrected in samples below these respective depths.¹

[10] Mg/Ca-temperature calibrations using core top material require accuracy in measurements of both the dependent variable (Mg/Ca) and the independent variable (temperature) and the assumption that the animal secreted its shell at the estimated temperature. Although we cannot totally exclude

short-term temperature changes at some sites, we are confident that the estimated bottom water temperatures were representative of the mean values at or near the sampling site for most core tops. In addition, many core top specimens were recently alive based on the preservation of appendages, Rose Bengal staining, and preservation of adult articulated carapaces. However, for several locations on the continental slope of the Southeast United States in the Florida Straits and Blake Plateau, bottom water temperature varies spatially and temporally due to the proximity to the Gulf Stream axis, complicating the attainment of bottom temperatures at the exact core top sites. These regions are also subject to bottom current erosion from interaction of the Gulf Stream with the seafloor such that some surface samples may include reworked or transported specimens [e.g., Kaneps, 1979]. We thus could not be confident in either the age of the ostracode specimens, or the temperature in which they secreted their calcitic shells, and excluded samples from the Florida Straits and Blake Plateau from the calibration equations for the North Atlantic.

3. Results

3.1. Water Column Profiles

[11] Profiles of Mg/Ca and Sr/Ca ratios from all *Krithe* core top specimens are plotted with temperature, salinity and $\Delta[\text{CO}_3^{2-}]$ for the North Atlantic and Nordic Seas/Arctic Ocean in Figures 2 and 3, respectively. The North Atlantic data show decreases in BWT, salinity and $\Delta[\text{CO}_3^{2-}]$ with depth in the uppermost 1000 m. Below 1000 m, temperatures remain near 2–5°C, salinity near 35, and $\Delta[\text{CO}_3^{2-}]$ near 50 $\mu\text{mol/kg}$ down to 3000 m, before reaching 0 $\mu\text{mol/kg}$ below 4000 m (Figures 2a–2c). Core top Mg/Ca (Figure 2d) mirrors the temperature, salinity and $\Delta[\text{CO}_3^{2-}]$ profiles with highest values in the upper 1000 m ($>20\ \text{mmol/mol}$), falling to ~ 6 – $10\ \text{mmol/mol}$ below 2000 m. There is a general depth gradient in Sr/Ca, with higher Sr/Ca values generally concentrated in the upper 1000 m and between 2000 and 3000 m, and lower values below 3000 m (Figure 2e).

[12] In the Arctic Ocean and Nordic Seas, mean annual temperatures are coldest in the Polar Surface Layer (down to -1.8°C) characteristic of our core top samples from the Kara and Laptev Seas. The warmest temperatures (0 – 2°C) reflect the Atlantic-sourced Arctic Intermediate Water, also called the Atlantic Layer [Rudels *et al.*, 2004], between 200 and 800 m (Figure 3a). Below 1000 m, water temperatures range from -0.75 to -1.0°C down to abyssal depths. Salinity is also lowest in the Polar Surface Layer, before rising to a nearly constant 34.9 below ~ 600 m (Figure 3b). $\Delta[\text{CO}_3^{2-}]$ displays consistent patterns in the Nordic Seas, and Arctic Eurasian and Amerasian Basins, with surface values close to 60 $\mu\text{mol/kg}$ and a steady decrease to carbonate-unsaturated water ($\Delta[\text{CO}_3^{2-}] < 0$) below approximately 4000 m (Figure 3c). Core top *Krithe* Mg/Ca values are lowest in the Polar Surface Layer, higher in the Atlantic Layer, and show a large amount of scatter below 1000 m depth (Figure 3d). *Krithe* Sr/Ca values show less scatter than in the North Atlantic but generally decrease with depth (Figure 3e).

[13] Figure 4 illustrates these relationships using cross-sections of temperature, $\Delta[\text{CO}_3^{2-}]$, and *Krithe* Mg/Ca and Sr/Ca data across the Nordic Seas and Arctic Ocean. *Krithe* Mg/Ca distribution is broadly consistent with the presence of

¹Auxiliary materials are available in the HTML. doi:10.1029/2012PA002305.

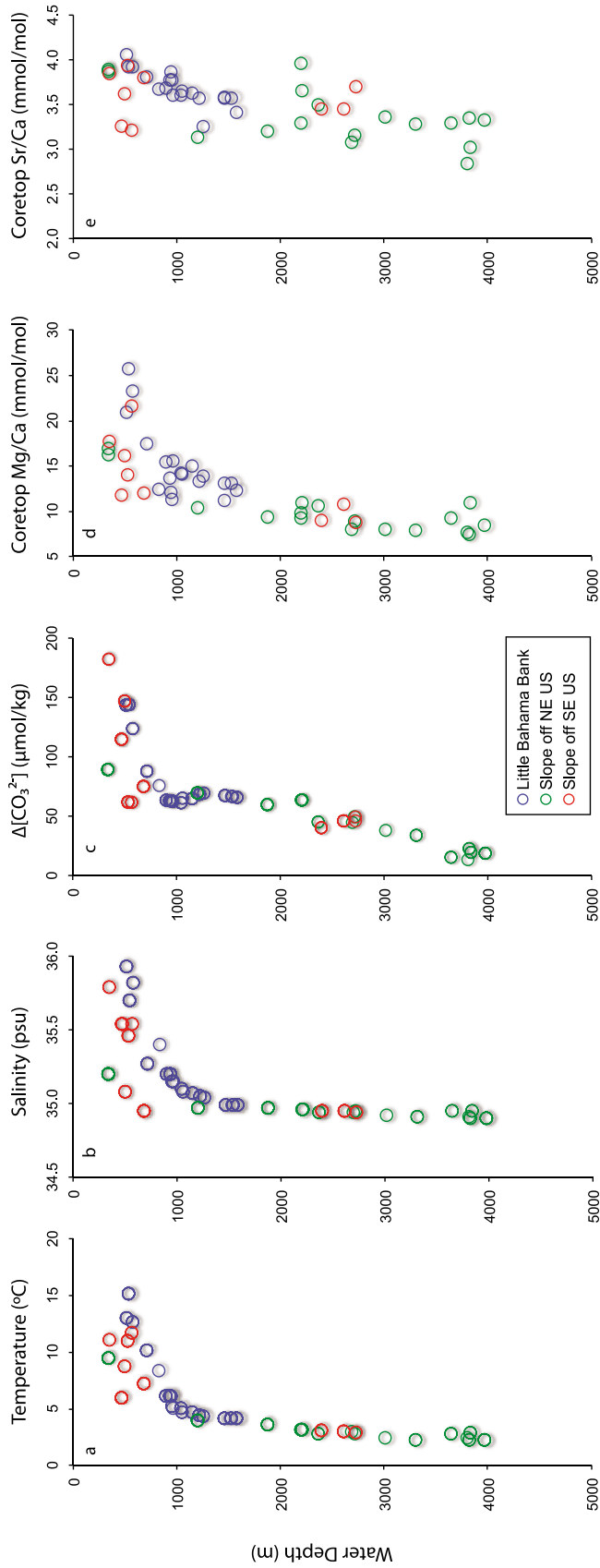


Figure 2. Water column profiles of (a) mean-annual temperature ($^{\circ}\text{C}$), (b) salinity (psu), and (c) preanthropogenic $\Delta[\text{CO}_3^{2-}]$ ($\mu\text{mol/kg}$) with (d) single-specimen core top *Kriehle* Mg/Ca (mmol/mol) and (e) Sr/Ca (mmol/mol) for North Atlantic Ocean samples. Blue circles are Little Bahama Bank samples, green circles are sites from the continental slope off the Northeastern United States (north of 37°N), and red circles are sites from the continental slope off the Southeastern United States (south of 37°N).

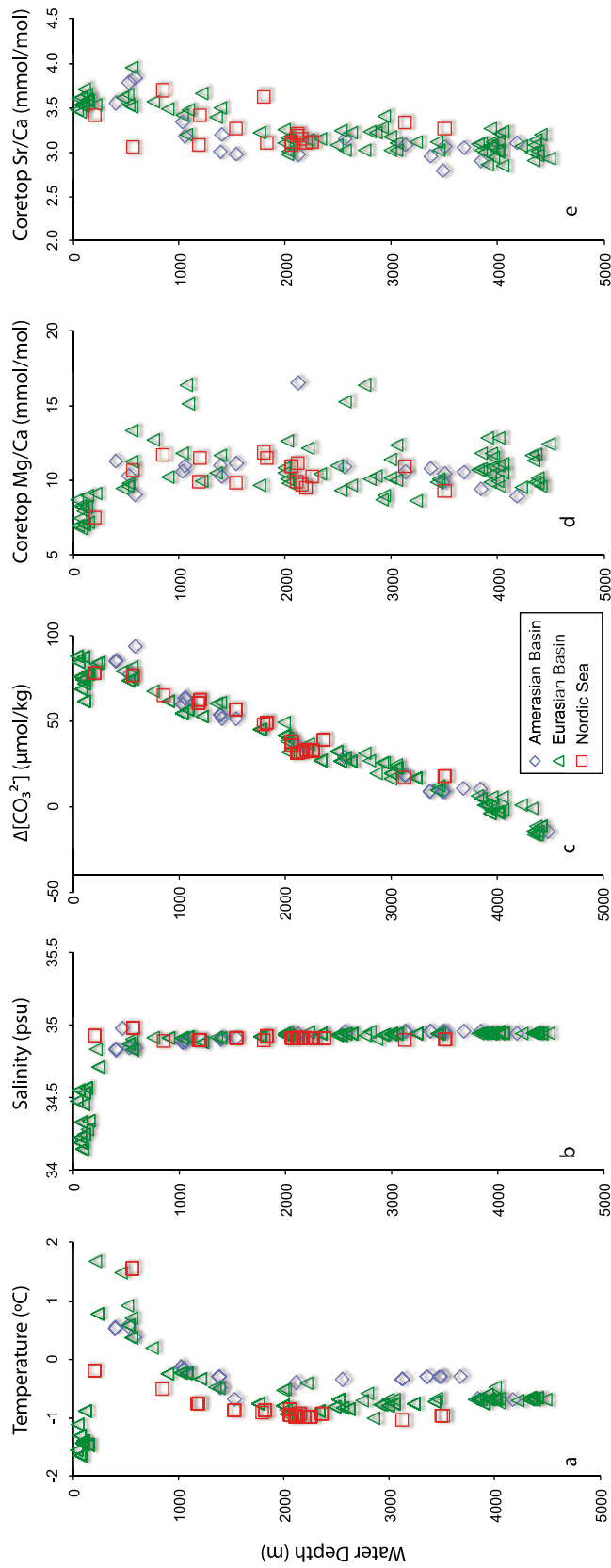


Figure 3. Water column profiles of (a) mean-annual temperature ($^{\circ}\text{C}$), (b) salinity (psu), and (c) preanthropogenic $\Delta[\text{CO}_3^{2-}]$ ($\mu\text{mol/kg}$) with (d) single-specimen core top *Kritho* Mg/Ca (mmol/mol) and (e) Sr/Ca (mmol/mol) for Arctic Ocean and Nordic Seas samples. Colors and shapes of symbols indicate different Arctic Basins; blue diamonds are Amerasian Basin, green triangles are Eurasian Basin, and red squares are Nordic Sea samples.

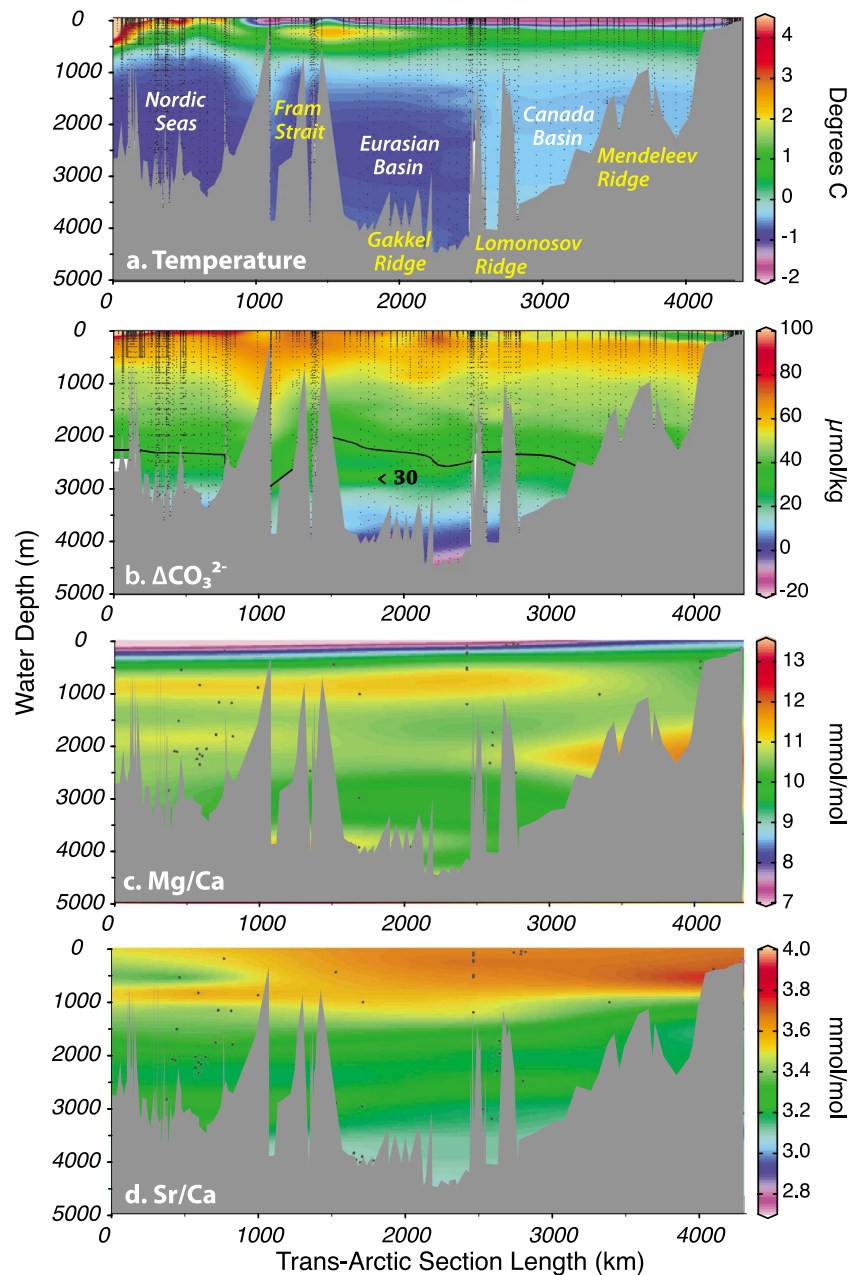


Figure 4. Transect across the Arctic Ocean and Nordic Seas showing (a) temperature, (b) modern $\Delta[\text{CO}_3^{2-}]$, (c) *Krithe glacialis* Mg/Ca and (d) Sr/Ca variability for core tops with greater than one specimen. Major bathymetric features are labeled in Figure 4a. Black points represent individual stations used for gridding. Black line in Figure 4b is 30 $\mu\text{mol/kg}$ threshold in $\Delta[\text{CO}_3^{2-}]$ below which a carbonate ion effect is observed in foraminiferal Zn/Ca [Marchitto *et al.*, 2000]. Physical data in Figures 4a and 4b are DIVA gridded with a 50 km \times 50 m window; trace metal data in Figures 4c and 4d are DIVA gridded with a larger 500 km \times 500 m window to account for coarser data spacing.

a cold Polar Surface Layer (lower Mg/Ca ratios), and a warm Atlantic Layer and downward mixing of Atlantic Layer heat especially in the Canada Basin (higher Mg/Ca values, Figure 4c). *Krithe* Sr/Ca is generally highest in the upper 1000 m, especially in the Canada Basin, and lower in the deep basins (Figure 4d). The variability in both trace metal ratios is modest below 1500 m (1–2 mmol/mol for Mg/Ca, 0.3 mmol/mol for Sr/Ca), and additional samples are needed

to ascertain whether small temperature changes and the larger $\Delta[\text{CO}_3^{2-}]$ gradient affect ratios in the deepest Arctic basins.

3.2. Calibration of Mg/Ca to Temperature

[14] Regression statistics for linear least squares fit of Mg/Ca to temperature for each *Krithe* species are summarized in Table 1. The results show a range of temperature sensitivities from 0.60 for *K. morkhoveni* to 1.67 mmol/mol per $^{\circ}\text{C}$

Table 1. Statistics for *Krithe* Mg/Ca Calibration Approaches

Single Species Least-Squares Calibrations							
Species	Equation Form	a	b	±95% CI, a	±95% CI, b	r ²	n
<i>aequalis</i>	Mg/Ca = a*T + b	0.79	8.65	0.53–1.05	6.85–10.45	0.38	62
ex. gr. <i>dolichodeira</i>	Mg/Ca = a*T + b	1.67	6.02	1.45–1.99	4.64–7.4	0.48	12
<i>glacialis</i>	Mg/Ca = a*T + b	1.07	10.88	0.73–1.41	10.58–11.18	0.13	268
<i>morkhovei</i>	Mg/Ca = a*T + b	0.6	8.09	0.36–0.84	6.89–9.29	0.40	38
<i>pernoides</i>	Mg/Ca = a*T + b	1.12	7.06	0.70–1.54	3.96–10.16	0.76	11
<i>reversa</i>	Mg/Ca = a*T + b	0.83	6.38	0.33–1.33	2.88–9.88	0.55	11
<i>trinidadensis</i>	Mg/Ca = a*T + b	1.28	4.75	1.12–1.44	4.15–5.35	0.98	8
species <i>x</i>	Mg/Ca = a*T + b	1.2	6.8	0.84–1.56	4.74–8.86	0.75	16
Regional Calibrations							
Curve Fit Type	Equation Form	a	b	95% CI, a	95% CI, b	r ²	rmse
<i>North Atlantic Specimens (n = 128)</i>							
LLS ^a	Mg/Ca = a*T + b	1.13	6.425	1.024–1.236	5.67–7.19	0.74	2.1
Exp ^b	Mg/Ca = b*exp(a*T)	0.074	8.191	0.068–0.08	7.72–8.67	0.75	2.2
RMA ^c	Mg/Ca = a*T + b	1.317	5.253	1.207–1.43	4.48–5.98	0.72	2.2
<i>Multispecimen Arctic Coretop Averages (n = 50)</i>							
LLS ^a	Mg/Ca = a*T + b	2.279	11.72	1.622–2.935	11.12–12.33	0.50	1.0
RMA ^c	Mg/Ca = a*T + b	3.211	12.48	2.593–3.941	11.73–12.97	0.43	1.1

^aLLS = Linear Least Squares.

^bExp = Exponential.

^cRMA = Reduced Major Axis.

for the *K. dolichodeira* species group, however overall Mg/Ca values are not demonstrably different between *Krithe* species. *Krithe glacialis* inhabits colder BWT common in the Arctic and Nordic Seas, while other *Krithe* species are distributed across broad temperature ranges in the North Atlantic (auxiliary material).

[15] Previous calibration studies of Mg/Ca and temperature in *Krithe* show regional variability in the Atlantic, Arctic, and Pacific oceans, suggesting that region-specific calibrations may be more appropriate for *Krithe* paleotemperature reconstructions than a single, unified global

calibration [Dwyer *et al.*, 1995; Cronin *et al.*, 1996; Corrège and De Deckker, 1997; Dwyer *et al.*, 2002]. Figure 5 shows Mg/Ca and BWT for North Atlantic and Arctic/Nordic Seas *Krithe*, with separate calibrations for each region. Mg/Ca and BWT from 158 *Krithe* samples at 46 locations in the North Atlantic and Little Bahama Banks are shown in Figure 5a. The linear least squares best fit to the North Atlantic data is given by:

$$\text{BWT}(^{\circ}\text{C}) = (0.885 \times \text{Mg/Ca}) - 5.69 \quad (1)$$

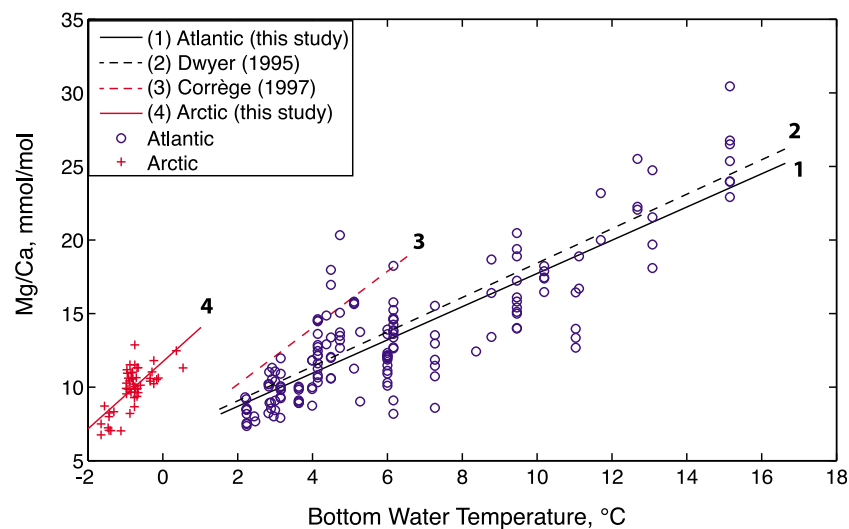


Figure 5. Linear least squares fit between North Atlantic core top Mg/Ca (blue circles, solid black line) and mean Mg/Ca from Arctic and Nordic Seas core tops with two or more specimens (red +', solid red line) to BWT. Also shown for comparison are the original North Atlantic calibration of Dwyer *et al.* [1995] (black dashed line) and the Coral Sea calibration of Corrège and De Deckker [1997] (red dashed line).

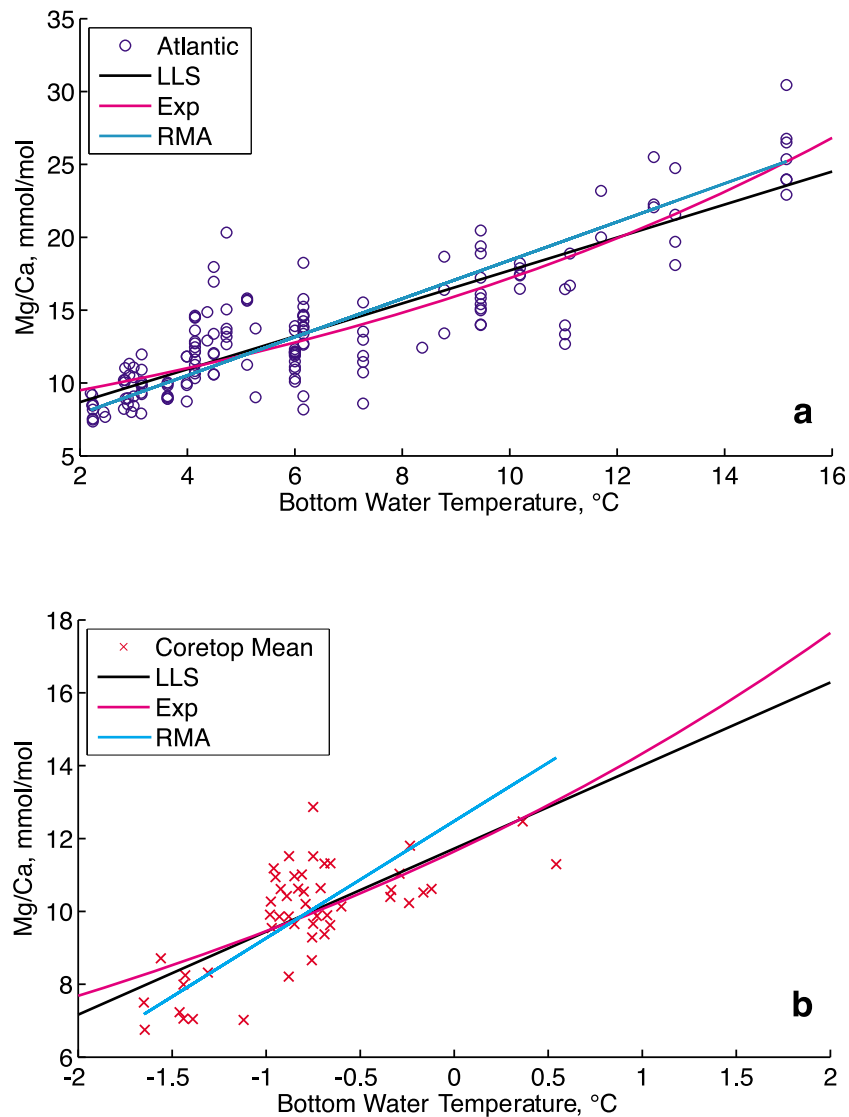


Figure 6. Calibration approaches between *Kriithe* Mg/Ca and BWT. (a) Linear least squares (LLS, black), one-term exponential (Exp, magenta), and reduced major axis least squares (RMA, cyan) for North Atlantic core top data (blue circles). (b) LLS, Exp and RMA calibrations to mean Mg/Ca from Arctic and Nordic core tops with two or more specimens (red x's). LLS fits are the same as those shown in Figure 5. Regression parameters are given in Table 1.

The standard error of prediction with this single specimen calibration is $\pm 2.1^{\circ}\text{C}$, but can be reduced by a factor of $1/(n)^{1/2}$ for n analyses. The slope and intercept of this regression are statistically indistinguishable from the regression of *Dwyer et al.* [1995]. Furthermore, the slope and intercept of the North Atlantic least squares fit is consistent with the individual species calibrations, with a temperature sensitivity that is within two standard errors of the sensitivity of five of the seven Atlantic species calibrations, and a regression intercept that is within two standard errors of the intercept of six of the seven Atlantic species calibrations (Table 1).

[16] For Nordic Seas and Arctic Ocean samples, we constructed a calibration using mean Mg/Ca values from multiple *Kriithe glacialis* samples for each core top. Plotting mean Mg/Ca data for those core tops from the Nordic Seas and

Arctic Ocean with multiple specimens against temperature returns a strong positive relationship with a linear least squares fit ($r^2 = 0.5$, Figure 5 and Table 1):

$$\text{BWT} (^{\circ}\text{C}) = (0.439 \times \text{Mg/Ca}) - 5.14 \quad (2)$$

The standard error of prediction with this calibration is $\pm 1.0^{\circ}\text{C}$, but because the calibration is constructed from sample means, the prediction error cannot be reduced with additional analyses. The temperature sensitivity of this relationship ($2.279 \text{ mmol mol}^{-1} \text{ }^{\circ}\text{C}^{-1}$) is nearly double that of the North Atlantic calibration, consistent with the empirical calibration of Coral Sea *Kriithe* from 2° to 6°C [Corrège and De Deckker, 1997].

[17] The sample averaging approach was chosen in consideration of the narrow range of temperature variability

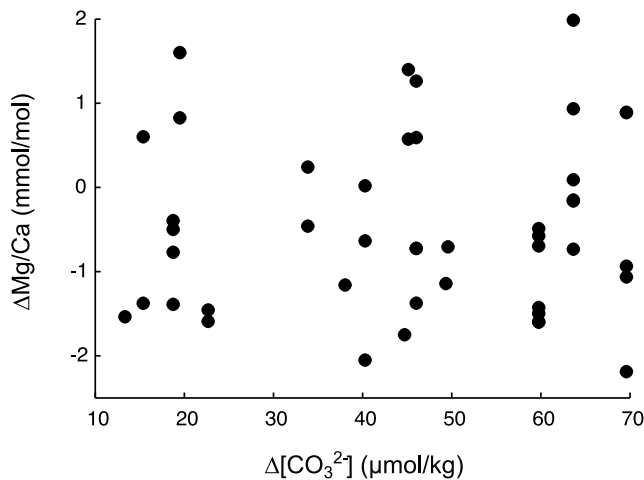


Figure 7. $\Delta\text{Mg}/\text{Ca}$ for between North Atlantic core top samples below 4°C and the North Atlantic linear least squares temperature calibration plotted against core top $\Delta[\text{CO}_3^{2-}]$ values.

within the Nordic/Arctic (-1.5 to 2°C), the presence of multiple *Krithe* specimens in many core tops, and the bulk analysis of multiple specimens from several Arctic core tops. Relatively few specimens of *K. glacialis* were available from the Atlantic Layer, probably reflecting its habitat preference for colder water temperatures found in the deep-sea and shallow Arctic shelf environments [Coles *et al.*, 1994; Poirier *et al.*, 2012]. Additional samples with high-quality core top specimens from the Atlantic Layer are needed to constrain the warmer end of our Arctic/Nordic calibration.

[18] In addition to linear least squares calibrations, we also fit exponential least squares and reduced major axis regressions to the North Atlantic and Arctic/Nordic core top data, respectively (Figure 6). For the North Atlantic, all three calibration approaches are similar, although the exponential fit explains the greatest percentage of shared variance (Table 1). For Arctic and Nordic Seas core tops, the linear and exponential least squares calibrations are indistinguishable across the temperature range in these core tops. A reduced major axis fit produces a larger temperature sensitivity of $3.211 \text{ mmol mol}^{-1} \text{ }^\circ\text{C}^{-1}$.

3.3. Carbonate Ion Saturation and *Krithe* Mg/Ca

[19] Elderfield *et al.* [2006] outlined a procedure for testing for the presence of a carbonate ion effect by assuming that a temperature effect on Mg/Ca is dominant above a temperature threshold, removing the temperature effect using Mg/Ca-temperature calibrations, and comparing the residual Mg/Ca (termed $\Delta\text{Mg}/\text{Ca}$ here) to $\Delta[\text{CO}_3^{2-}]$. We evaluate the possibility of a carbonate ion effect on North Atlantic and Arctic *Krithe* Mg/Ca using this method, assuming that the North Atlantic temperature-Mg/Ca calibrations represent temperature dependent Mg/Ca variability. Figure 7 shows that $\Delta\text{Mg}/\text{Ca}$ values for North Atlantic samples with core top temperatures below 4°C show no relationship to $\Delta[\text{CO}_3^{2-}]$ using the linear least squares relationship to define the effect of temperature on Mg/Ca. For the Arctic Ocean and Nordic Seas samples, $\Delta\text{Mg}/\text{Ca}$ values are greater than zero for all samples using the linear least

squares North Atlantic calibration, showing that all analyzed specimens have greater Mg/Ca than expected at that temperature using the North Atlantic linear least squares calibration (Figure 8). Further, $\Delta\text{Mg}/\text{Ca}$ values show no relationship to core top $\Delta[\text{CO}_3^{2-}]$ for our extensive set of *Krithe* Mg/Ca data from the Nordic Seas and Arctic Ocean (Figure 8b). For convenience, only $\Delta\text{Mg}/\text{Ca}$ values calculated using least squares linear and exponential North Atlantic calibrations are shown, but a lack of relationship between $\Delta\text{Mg}/\text{Ca}$ and $\Delta[\text{CO}_3^{2-}]$ can be shown for all of the regression approaches in Table 1.

4. Discussion

4.1. Comparison of Calibration Approaches

[20] Previous studies of Mg/Ca in *Krithe* have shown that trace metal variability is influenced more by ontogenetic rather than inter-specific variability [Dwyer *et al.*, 1995, 2002]. Our analyses of adult specimens also suggest that the molar Mg concentration is not variable across *Krithe*

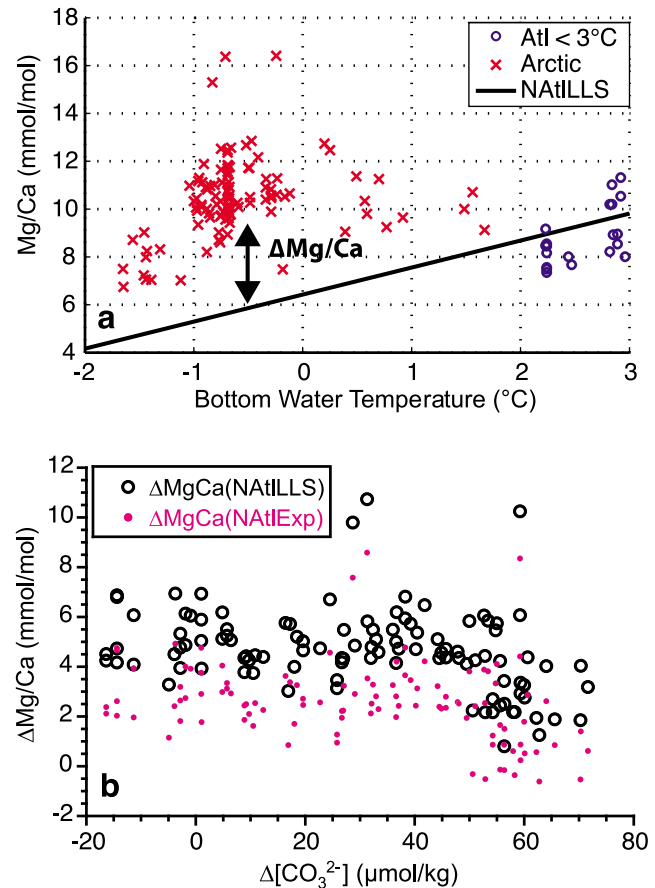


Figure 8. (a) Mg/Ca values for Arctic *Krithe* (red x's) compared to extrapolation of the North Atlantic linear least squares calibration line (black). North Atlantic *Krithe* Mg/Ca for core tops below 3°C are shown for comparison (blue circles). The offset of Arctic and Nordic Seas Mg/Ca values from the calibration line is termed $\Delta\text{Mg}/\text{Ca}$ (arrow). (b) $\Delta\text{Mg}/\text{Ca}$ for linear least squares (black circles) and exponential (magenta points) North Atlantic calibrations versus core top $\Delta[\text{CO}_3^{2-}]$ values.

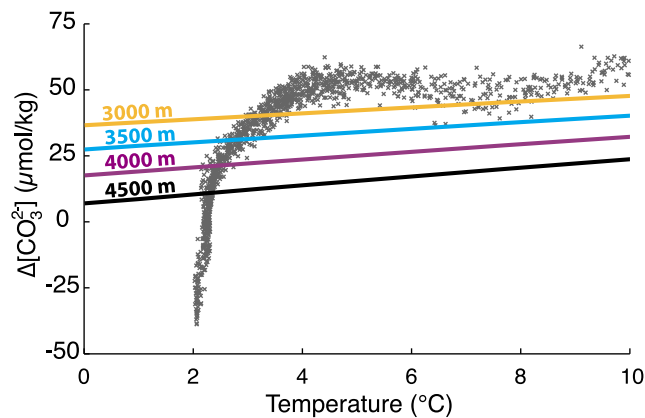


Figure 9. Temperature versus $\Delta[\text{CO}_3^{2-}]$ for samples from the western North Atlantic (22° to 45°N , 60° to 80°W) in the CARINA data set. Colored lines represent the thermo-dependence of $\Delta[\text{CO}_3^{2-}]$ calculated from the CO2sys program using fixed salinity, alkalinity and DIC. The slopes of the temperature- $\Delta[\text{CO}_3^{2-}]$ relationships are approximately $1 \mu\text{mol/kg per } ^\circ\text{C}$.

species, implying that temperature is more dominant than inter-specific processes in determining *Krithe* Mg/Ca. Calibrations between the Mg/Ca of each *Krithe* species and temperature (Table 1 and auxiliary material) show a three-fold range in temperature sensitivities, which we cannot rule out as distinct species differences. The threefold range in temperature sensitivities for *Krithe* is similar to the range in sensitivities observed for different species of the cosmopolitan benthic foraminifer *Cibicidoides* [Elderfield et al., 2006; Bryan and Marchitto, 2008], although distinct offsets are observed in molar Mg concentration between *Cibicidoides* species [Healey et al., 2008]. For paleotemperature reconstructions, the potential for inter-specific differences in the temperature sensitivity of Mg incorporation with *Krithe* is likely a secondary consideration compared to variability in *Krithe* species assemblages and the preservation of *Krithe* specimens in downcore records [Dwyer et al., 1995; Cronin et al., 1999, 2000; Dwyer et al., 2000, 2002]. As a result, with the exception of *K. glacialis* for the Arctic, we consider the individual species calibrations less useful for paleotemperature reconstruction than the regional calibrations (Figures 5 and 6).

[21] The three calibration approaches presented here (linear least squares, exponential least squares, and reduced major axis) are included because of uncertainty surrounding the most appropriate form of the Mg/Ca-temperature relationship for paleotemperature applications. Inorganic precipitation experiments and culturing studies of planktonic foraminifers have argued that Mg partitioning into calcite is exponentially related to water temperature [e.g., Oomori et al., 1987; Lea et al., 1999]; other studies have presented linear models to account for the observed empirical relationship between Mg/Ca in biogenic carbonate and temperature [e.g., Chave, 1954; Dwyer et al., 1995; Bryan and Marchitto, 2008]. A second area of discussion revolves on the most appropriate type of statistical regression. Least squares regression assumes that all error is contained within the dependent variable (Mg/Ca), but temperature measurements used for

calibration are also subject to uncertainty, and thus the most statistically appropriate form of calibration is reduced major axis [Rosenthal and Lohmann, 2002]. Generally, reduced major axis regressions to our *Krithe* data return higher temperature sensitivities than linear least squares, although these estimates are within 95% confidence of each other. The differences between calibration approaches are, from a statistical standpoint, minor, and we generally favor linear least squares approaches for consistency with previous studies (Table 1).

4.2. *Krithe* Mg/Ca Variability and Salinity

[22] In addition to temperature, there is a salinity gradient with depth in the North Atlantic (Figure 2) and Nordic Seas/Arctic Ocean (Figure 3). Although correspondence between salinity and trace metal ratios has been observed in planktonic foraminifera [e.g., Arbuszewski et al., 2010], it is unlikely that salinity is a primary factor for *Krithe* Mg/Ca for several reasons. First, the absolute salinity range for our core tops is minor (35 to 36 in the Atlantic, 34 to 35 in the Arctic) compared to the range of observed *Krithe* Mg/Ca values (6 to 27 mmol/mol in the Atlantic, 6 to 17 mmol/mol in the Arctic) (Figures 2 and 3). Second, culturing studies in the marine ostracode *Loxococoncha matgordensis* showed no relationship between Mg/Ca and salinity [Dwyer et al., 2002]. Third, if the positive relationship between salinity and Mg/Ca indicated a causal process, we would expect greater Mg/Ca values during glacial intervals, when the deep ocean was likely saltier [Adkins et al., 2002]. However, downcore reconstructions of Mg/Ca in North Atlantic *Krithe* show lower Mg/Ca values during glacial intervals [Dwyer et al., 1995, 2000].

4.3. *Krithe* Mg/Ca Variability and $\Delta[\text{CO}_3^{2-}]$

[23] The degree of carbonate ion saturation, $\Delta[\text{CO}_3^{2-}]$, has previously been shown to influence the partition coefficients of trace metals into benthic foraminiferal tests below around 3°C , or at $\Delta[\text{CO}_3^{2-}]$ values approaching saturation [McCorkle et al., 1995; Marchitto et al., 2000; Martin et al., 2002; Elderfield et al., 2006; Rosenthal et al., 2006; Yu and Elderfield, 2008]. In core top calibrations, the presence of a carbonate ion effect has been inferred from either a steeper Mg/Ca-temperature slope (e.g., a higher temperature sensitivity), or Mg/Ca values depleted below those expected at a given temperature from Mg/Ca-temperature regressions covering broader temperature ranges [Elderfield et al., 2006]. Previous research on *Krithe* samples from the Ontong Java plateau showed that Mg/Ca changes occurred in concert with temperature and carbonate saturation changes [Dwyer et al., 2002], but the possibility of a carbonate ion effect on *Krithe* Mg/Ca could not be isolated.

[24] Figure 2 shows that trends in core top Mg/Ca values from the North Atlantic generally track both temperature and $\Delta[\text{CO}_3^{2-}]$ in the water column. Whether Mg/Ca ratios are responding to $\Delta[\text{CO}_3^{2-}]$ or temperature is complicated by the documented positive relationship between these two parameters in the North Atlantic [Rosenthal et al., 2006]. $\Delta[\text{CO}_3^{2-}]$ is thermodynamically controlled through the temperature dependence of carbonate speciation equilibrium constants (see Appendix), however the influence of temperature on $\Delta[\text{CO}_3^{2-}]$ is generally minor ($\sim 1 \mu\text{mol/kg per } ^\circ\text{C}$, Figure 9) compared with the influence of non-temperature

factors (namely, alkalinity, DIC, and depth). *Elderfield et al.* [2006] noted that the slope of the $\Delta[\text{CO}_3^{2-}]$:temperature relationship steepens greatly below about 3°C. We observe that the $\Delta[\text{CO}_3^{2-}]$:temperature relationship becomes offset from the expected thermodynamic relationship by $\sim 4^\circ\text{C}$ in the North Atlantic (Figure 9), suggesting that, below this temperature, changes in $\Delta[\text{CO}_3^{2-}]$ are likely driven by variability in alkalinity and DIC. Although $\Delta[\text{CO}_3^{2-}]$ is no longer primarily thermodynamically controlled below 4°C, the $\Delta\text{Mg}/\text{Ca}$ approach shows that the offset in Mg/Ca values of our core top samples from the temperature calibration line is not a function of the carbonate saturation state (Figure 7). This is corroborated by the fact that Mg/Ca values for *Krithe* do not appear to show a systematic offset from the temperature calibration below 4°C (Figure 5), as is observed in some benthic foraminifers [*Elderfield et al.*, 2006]. As a result, we conclude that there is no apparent carbonate ion saturation effect on Mg/Ca ratios of *Krithe* in the North Atlantic down to 4000 m, our deepest core top site.

[25] The Arctic Ocean and Nordic Seas appear to be an ideal place to test for the presence of a carbonate ion effect, as they are uniformly cold (below 3°C) and show a large range in carbonate saturation states relative to minor temperature changes (Figure 3). The Arctic Ocean and Nordic Seas *Krithe* Mg/Ca data exhibit a steeper temperature sensitivity (Figure 5) in comparison to the North Atlantic calibrations, a trait associated with a carbonate ion effect in the benthic foraminifer *Cibicides wuellerstorfi* [*Elderfield et al.*, 2006]. However, the offset between observed Mg/Ca values and the North Atlantic Mg/Ca-temperature calibrations shows no relationship to $\Delta[\text{CO}_3^{2-}]$ (Figure 8b), leading us to conclude that Mg/Ca deviations in *Krithe* specimens from the Nordic Seas and Arctic Ocean cannot be attributed to changes in $\Delta[\text{CO}_3^{2-}]$. It is noteworthy that *Elderfield et al.* [2006] observed higher than expected Mg/Ca in their Nordic Seas benthic foraminifers, which they attributed to higher deepwater $\Delta[\text{CO}_3^{2-}]$. We also see higher than expected Mg/Ca in Nordic Seas and Arctic Ocean *Krithe* (Figure 8a), but this pattern persists across a range of $\Delta[\text{CO}_3^{2-}]$ values down to, and below, saturation (Figure 8b).

[26] The lack of evidence for a carbonate ion effect shown here might reflect a habitat preference (infaunal versus epifaunal) for *Krithe*. Some authors suggest a shallow (~ 1 cm) infaunal habitat for *Krithe* based on shell morphology [*Coles et al.*, 1994], and culturing of juvenile *Krithe* from shallow Swedish fjords [*Majoran and Agrenius*, 1995]. However, there is evidence that *Krithe* molts epifaunally, with shell chemistry thus recording bottom water conditions [*Dwyer et al.*, 2002]. Given an infaunal habitat for *Krithe*, no relationship would be expected *Krithe* Mg/Ca and bottom water $\Delta[\text{CO}_3^{2-}]$, as the carbonate saturation state of pore waters is dependent on sediment properties (accumulation rate, % organics, etc.), and thus unrelated to bottom water $\Delta[\text{CO}_3^{2-}]$ [*Elderfield et al.*, 2006, 2010]. Conversely, for an epifaunal habitat, the lack of a carbonate ion effect in North Atlantic, Nordic Seas and Arctic *Krithe* would suggest that Mg partitioning during the shell secretion process occurs independent of carbonate ion saturation. In sum, it is unknown whether all *Krithe* species share an infaunal habitat, or even whether an infaunal habitat is constant across the lifetime of an individual *Krithe*.

[27] If carbonate ion saturation does not relate to *Krithe* Mg/Ca variability, then what can account for the higher temperature sensitivity and relatively higher Mg/Ca in the Arctic Ocean than the North Atlantic? The higher temperature sensitivity of Arctic and Nordic *Krithe* Mg/Ca is not unusual for ostracodes, considering the range of sensitivities shown in previously published *Krithe* calibrations from the Pacific Ocean [*Corrège*, 1993; *Corrège and De Deckker*, 1997], North Atlantic [*Dwyer et al.*, 1995, 2002], and Arctic [*Cronin et al.*, 1996]. Elevated Mg/Ca ratios in Arctic and Nordic Seas *Krithe* from intermediate and deep waters are inconsistent with reduced $\Delta[\text{CO}_3^{2-}]$ at these depths, as decreased $\Delta[\text{CO}_3^{2-}]$ should cause a reduction in Mg/Ca ratios [*Elderfield et al.*, 2006]. The partitioning of Mg in ostracode calcite also may depend on factors other than temperature, such as nutrient availability and calcification rate [*Dwyer et al.*, 1995; *Corrège and De Deckker*, 1997; *Dwyer et al.*, 2002]. Since *Krithe* assemblages in the Nordic Seas and Arctic Ocean are dominated by a single species, *Krithe glacialis*, we favor the possibility that *K. glacialis* physiology and shell secretion are adapted to counter extreme conditions for shell growth in the Arctic Ocean (below-zero temperatures and limited food supply) that alters Mg partitioning compared to North Atlantic *Krithe*. This hypothesis could best be tested through culturing studies of *Krithe glacialis* populations known to inhabit fjord regions of Sweden and Norway.

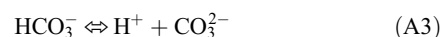
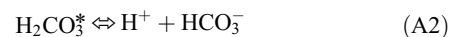
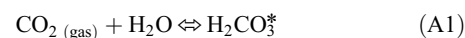
5. Conclusions

[28] We show that Mg/Ca ratios in eight species of the marine benthic ostracode genus *Krithe* are positively and linearly correlated to bottom water temperature in the North Atlantic Ocean ($\text{BWT} = (0.885 \times \text{Mg}/\text{Ca}) - 5.69$) and Nordic Seas and Arctic Ocean ($\text{BWT} = (0.439 \times \text{Mg}/\text{Ca}) - 5.14$). The calibration equation for *K. glacialis* from the Nordic/Arctic Seas shows a temperature sensitivity twice that of most North Atlantic species. We do not find evidence for a carbonate ion effect in *Krithe* Mg/Ca from the North Atlantic Ocean, Nordic Seas, and Arctic Ocean. Additional samples from the deep North Atlantic Ocean and the Atlantic Layer in the Arctic Ocean would improve our Mg/Ca-temperature calibrations in temperatures from 0 to 4°C.

Appendix A

A1. Calculating $[\text{CO}_3^{2-}]$

[29] The inorganic solution chemistry of CO_2 in seawater is based on the dissolution of CO_2 gas into seawater, and the resulting dissociation to bicarbonate (HCO_3^-) and carbonate (CO_3^{2-}) ions. These dissociations are described by three equilibrium reactions [*Dickson and Goyet*, 1994; *Sarmiento and Gruber*, 2006a]:



where H_2CO_3^* represents the combination of aqueous CO_2 and carbonic acid (H_2CO_3), which are difficult to distinguish analytically [Dickson and Goyet, 1994]. Each reaction is assigned an equilibrium constant based on the concentration of products versus reactants:

$$K_0 = [\text{H}_2\text{CO}_3^*]/p\text{CO}_2 \quad (\text{A4})$$

$$K_1 = [\text{H}^+][\text{HCO}_3^-]/[\text{H}_2\text{CO}_3^*] \quad (\text{A5})$$

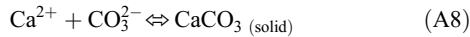
$$K_2 = [\text{H}^+][\text{CO}_3^{2-}]/[\text{HCO}_3^-] \quad (\text{A6})$$

K_0 through K_2 are functions of temperature and salinity in the global ocean [Sarmiento and Gruber, 2006a]. (Equations A4)–(A6) can be rearranged in terms of $[\text{H}^+]$ and $p\text{CO}_2$ to solve directly for $[\text{CO}_3^{2-}]$:

$$[\text{CO}_3^{2-}] = (K_0^*K_1^*K_2^*p\text{CO}_2)/[\text{H}^+]^2 \quad (\text{A7})$$

A2. Calculating $[\text{CO}_3^{2-}]_{\text{sat}}$ and $\Delta[\text{CO}_3^{2-}]$

[30] The saturation concentration of carbonate ion ($[\text{CO}_3^{2-}]_{\text{sat}}$) for calcite can be determined using equations defining inorganic calcite solubility in seawater. The precipitation of inorganic calcite in seawater is given by the following reaction:



The solubility product for (A8) is given by:

$$K_{\text{sp}} = [\text{CO}_3^{2-}]_{\text{sat}} [\text{Ca}^{2+}]_{\text{sat}} \quad (\text{A9})$$

where $[\text{CO}_3^{2-}]_{\text{sat}}$ and $[\text{Ca}^{2+}]_{\text{sat}}$ are the concentrations of dissolved carbonate ion and calcium ion in equilibrium with CaCO_3 . The degree of saturation of calcite, Ω_{calcite} , is then the ratio between the observed concentrations of carbonate ion and calcium ion divided by their saturation concentrations:

$$\Omega_{\text{calcite}} = ([\text{CO}_3^{2-}] * [\text{Ca}^{2+}]) / ([\text{CO}_3^{2-}]_{\text{sat}} * [\text{Ca}^{2+}]_{\text{sat}})_{\text{calcite}} \quad (\text{A10})$$

The concentration of calcium ions in seawater is about three orders of magnitude larger than $[\text{CO}_3^{2-}]$, so processes influencing the formation and dissolution of carbonates have a correspondingly minor influence on $[\text{Ca}^{2+}]$ [Sarmiento and Gruber, 2006b]. Therefore, we can assume that $[\text{Ca}^{2+}]$ is approximately constant, reducing (A10) to:

$$\Omega_{\text{calcite}} = [\text{CO}_3^{2-}] / [\text{CO}_3^{2-}]_{\text{sat}} \quad (\text{A11})$$

Since $\Delta[\text{CO}_3^{2-}] = [\text{CO}_3^{2-}] - [\text{CO}_3^{2-}]_{\text{sat}}$, $\Delta[\text{CO}_3^{2-}]$ can be calculated using knowledge of $p\text{CO}_2$, $[\text{H}^+]$, K_0 , K_1 , K_2 (A7) and Ω_{calcite} (equation (A11)).

A3. Obtaining Values for Calculating $\Delta[\text{CO}_3^{2-}]$

[31] As shown above, the inorganic carbon system consists of a system of equations and unknowns. In order to completely define the system, two unknowns must be

specified [Sarmiento and Gruber, 2006a]. Four parameters are commonly measured: total alkalinity, total dissolved inorganic carbon, $p\text{CO}_2$ (or $f\text{CO}_2$), and pH. Of these four, any two, along with temperature, salinity, pressure, and relevant equilibrium constants, can be used to completely determine the inorganic carbon system using the CO2sys program [Lewis and Wallace, 1998]. CO2sys returns values for $[\text{CO}_3^{2-}]$ and Ω_{calcite} , from which $[\text{CO}_3^{2-}]_{\text{sat}}$ and $\Delta[\text{CO}_3^{2-}]$ can be determined using equation (A11). The sources for values for alkalinity, DIC, temperature, salinity, and the relevant equilibrium constants are given in section 2.

[32] **Acknowledgments.** We are thankful to J. Bernhard, E. Roosen, and the crew of R/V *Oceanus* Expedition 461 for assistance with sample collection; A. Stepanova and W. M. Briggs Jr. for specimens; and L. Gemery, R. Glazer, and R. Poirier for laboratory assistance. We thank Y. Rosenthal and A. Elmore for helpful discussions and Editor R. Zahn and two anonymous reviewers for their insightful comments that greatly improved the manuscript. This work was funded by the USGS Global Change Research and Development Program.

References

- Adkins, J. F., K. McIntyre, and D. P. Schrag (2002), The salinity, temperature, and $\delta^{18}\text{O}$ of the glacial deep ocean, *Science*, 298, 1769–1773, doi:10.1126/science.1076252.
- Arbuszewski, J., P. deMenocal, A. Kaplan, and E. C. Farmer (2010), On the fidelity of shell-derived $\delta^{18}\text{O}_{\text{seawater}}$ estimates, *Earth Planet. Sci. Lett.*, 300, 185–196, doi:10.1016/j.epsl.2010.10.035.
- Bamberg, A., Y. Rosenthal, A. Paul, D. Heslop, S. Mulitza, C. Rühlemann, and M. Schulz (2010), Reduced North Atlantic Central Water formation in response to early Holocene ice-sheet melting, *Geophys. Res. Lett.*, 37, L17705, doi:10.1029/2010GL043878.
- Bohaty, S. M., J. C. Zachos, and M. L. Delaney (2012), Foraminiferal Mg/Ca evidence for Southern Ocean cooling across the Eocene-Oligocene transition, *Earth Planet. Sci. Lett.*, 317–318, 251–261, doi:10.1016/j.epsl.2011.11.037.
- Boyer, T. P., C. Stephens, J. I. Antonov, M. E. Conkright, R. A. Locarnini, T. D. O'Brien, and H. E. Garcia (2002), *World Ocean Atlas 2001*, vol. 2, *Salinity*, NOAA Atlas NESDIS, vol. 50, NOAA, Silver Spring, Md.
- Broecker, W., and J. Yu (2011), What do we know about the evolution of Mg to Ca ratios in seawater?, *Paleoceanography*, 26, PA3203, doi:10.1029/2011PA002120.
- Bryan, S. P., and T. M. Marchitto (2008), Mg/Ca-temperature proxy in benthic foraminifera: New calibrations from the Florida Straits and a hypothesis regarding Mg/Li, *Paleoceanography*, 23, PA2220, doi:10.1029/2007PA001553.
- Chave, K. E. (1954), Aspects of the biogeochemistry of magnesium, 1: Calcareous marine organisms, *J. Geol.*, 62, 266–283, doi:10.1086/626162.
- Chivas, A. R., P. De Deckker, and J. M. G. Shelley (1986), Magnesium content of non-marine ostracod Shells: A new palaeosalinometer and palaeothermometer, *Palaeogeogr. Palaeoclimatol. Palaeoecol.*, 54, 43–61, doi:10.1016/0031-0182(86)90117-3.
- Chivas, A. R., P. De Deckker, J. A. Cali, A. Chapman, E. Kiss, and J. M. G. Shelley (1993), Coupled stable-isotope and trace-element measurements of lacustrine carbonates as paleoclimatic indicators, in *Climate Change in Continental Isotopic Records*, *Geophys. Monogr. Ser.*, vol. 78, edited by P. K. Swart et al., pp. 113–121, AGU, Washington, D. C., doi:10.1029/GM078p0113.
- Coggon, R. M., D. A. H. Teagle, C. E. Smith-Duque, J. C. Alt, and M. J. Cooper (2010), Reconstructing past seawater Mg/Ca and Sr/Ca from mid-ocean ridge flank calcium carbonate veins, *Science*, 327, 1114–1117, doi:10.1126/science.1182252.
- Coles, G. P., R. C. Whatley, and A. Muguilevsky (1994), The ostracod genus *Krithe* from the Tertiary and Quaternary of the North Atlantic, *Palaeontology*, 37, 71–120.
- Corrège, T. (1993), Preliminary results of paleotemperature reconstruction using the magnesium to calcium ratio of deep-sea ostracode shells from the late Quaternary of Site 822, Leg 133 (western Coral Sea), *Proc. Ocean Drill. Program Sci. Results*, 133, 175–180.
- Corrège, T., and P. De Deckker (1997), Faunal and geochemical evidence for changes in intermediate water temperature and salinity in the western Coral Sea (northeast Australia) during the Late Quaternary, *Palaeogeogr. Palaeoclimatol. Palaeoecol.*, 131, 183–205, doi:10.1016/S0031-0182(97)00003-5.

- Cronin, T. M., G. S. Dwyer, P. A. Baker, J. Rodriguez-Lazaro, and W. M. Briggs Jr. (1996), Deep-sea ostracode shell chemistry (Mg:Ca ratios) and late Quaternary Arctic Ocean history, in *Late Quaternary Paleoceanography of North Atlantic Margins*, edited by J. T. Andrews et al., *Geol. Soc. Spec. Publ.*, 111, 117–134.
- Cronin, T. M., D. M. DeMartino, G. S. Dwyer, and J. Rodriguez-Lazaro (1999), Deep-sea ostracode species diversity: Response to late Quaternary climate change, *Mar. Micropaleontol.*, 37, 231–249, doi:10.1016/S0377-8398(99)00026-2.
- Cronin, T. M., G. S. Dwyer, P. A. Baker, J. Rodriguez-Lazaro, and D. M. DeMartino (2000), Orbital and suborbital variability in deep North Atlantic bottom water temperature obtained from Mg/Ca ratios in the ostracode *Krihe*, *Palaeogeogr. Palaeoclimatol. Palaeoecol.*, 162, 45–57, doi:10.1016/S0031-0182(00)00104-8.
- Cronin, T. M., T. Kamiya, G. S. Dwyer, H. Belkin, C. D. Vann, S. Schwede, and R. Wagner (2005a), Ecology and shell chemistry of *Loxococoncha matagordensis*, *Palaeogeogr. Palaeoclimatol. Palaeoecol.*, 225, 14–67, doi:10.1016/j.palaeo.2005.05.022.
- Cronin, T. M., H. J. Dowsett, G. S. Dwyer, P. A. Baker, and M. A. Chandler (2005b), Mid-Pliocene deep-sea bottom-water temperatures based on ostracode Mg/Ca ratios, *Mar. Micropaleontol.*, 54, 249–261, doi:10.1016/j.marmicro.2004.12.003.
- De Deckker, P., A. R. Chivas, and J. M. G. Shelley (1999), Uptake of Mg and Sr in the euryhaline ostracod *Cyprideis* determined from in vitro experiments, *Palaeogeogr. Palaeoclimatol. Palaeoecol.*, 148, 105–116, doi:10.1016/S0031-0182(98)00178-3.
- Dickson, A. G. (1990), Standard potential of the $(\text{AgCl(s)} + \frac{1}{2}\text{H}_2(\text{g}) = \text{Ag(s)} + \text{HCl(aq)})$ cell and the dissociation constant of bisulfate ion in synthetic sea water from 273.15 to 318.15 K, *J. Chem. Thermodyn.*, 22, 113–127, doi:10.1016/0021-9614(90)90074-Z.
- Dickson, A. G., and C. Goyet (1994), Solution chemistry of carbon dioxide in sea water, in *Handbook of Methods for the Analysis of the Various Parameters of the Carbon Dioxide System in Sea Water*, Rep. ORNL/CDIAC-74, Oak Ridge Natl. Lab., Oak Ridge, Tenn.
- Dickson, A. G., and F. J. Millero (1987), A comparison of the equilibrium constants for the dissociation of carbonic acid in seawater media, *Deep Sea Res., Part A*, 34, 1733–1743, doi:10.1016/0198-0149(87)90021-5.
- Dwyer, G. S., and M. A. Chandler (2009), Mid-Pliocene sea level and continental ice volume based on coupled benthic Mg/Ca palaeotemperatures and oxygen isotopes, *Philos. Trans. R. Soc. A*, 367, 157–168, doi:10.1098/rsta.2008.0222.
- Dwyer, G. S., T. M. Cronin, P. A. Baker, M. E. Raymo, J. Buzas, and T. Corrége (1995), North Atlantic deepwater temperature change during Late Pliocene and Late Quaternary climatic cycles, *Science*, 270, 1347–1351, doi:10.1126/science.270.5240.1347.
- Dwyer, G. S., T. M. Cronin, P. A. Baker, and J. Rodriguez-Lazaro (2000), Changes in North Atlantic deep-sea temperature during climatic fluctuations of the last 25,000 years based on ostracode Mg/Ca ratios, *Geochem. Geophys. Geosyst.*, 1, 1028, doi:10.1029/2000GC000046.
- Dwyer, G. S., T. M. Cronin, and P. A. Baker (2002), Trace elements in marine ostracodes, in *The Ostracoda: Applications in Quaternary Research*, *Geophys. Monogr. Ser.*, vol. 131, edited by J. A. Holmes and A. R. Chivas, pp. 205–225, AGU, Washington, D. C., doi:10.1029/131GM11.
- Elderfield, H., J. Yu, P. Anand, T. Kiefer, and B. Nyland (2006), Calibrations for benthic foraminiferal Mg/Ca paleothermometry and the carbonate ion hypothesis, *Earth Planet. Sci. Lett.*, 250, 633–649, doi:10.1016/j.epsl.2006.07.041.
- Elderfield, H., M. Greaves, S. Barker, I. R. Hall, A. Tripathi, P. Ferretti, S. Crowhurst, L. Booth, and C. Daut (2010), A record of bottom water temperature and seawater $\delta^{18}\text{O}$ for the Southern Ocean over the past 440 kyr based on Mg/Ca of benthic foraminiferal *Uvigerina* spp., *Quat. Sci. Rev.*, 29, 160–169, doi:10.1016/j.quascirev.2009.07.013.
- Garcia, H. E., R. A. Locarnini, T. P. Boyer, and J. I. Antonov (2010), *World Ocean Atlas 2009*, vol. 4, *Nutrients (Phosphate, Nitrate, and Silicate)*, NOAA Atlas NESDIS, vol. 71, edited by S. Levitus, 396 pp., NOAA, Silver Spring, Md.
- Healey, S. L., R. C. Thunell, and B. H. Corliss (2008), The Mg/Ca-temperature relationship of benthic foraminiferal calcite: New core-top calibrations in the $<4^\circ\text{C}$ temperature range, *Earth Planet. Sci. Lett.*, 272, 523–530, doi:10.1016/j.epsl.2008.05.023.
- Holmes, J. A., and A. R. Chivas (2002), Ostracod shell chemistry — overview, in *The Ostracoda: Applications in Quaternary Research*, *Geophys. Monogr. Ser.*, vol. 131, edited by J. A. Holmes and A. R. Chivas, pp. 185–204, AGU, Washington, D. C., doi:10.1029/131GM10.
- Kaneps, A. G. (1979), Gulf Stream: Velocity fluctuations during the Late Cenozoic, *Science*, 204, 297–301, doi:10.1126/science.204.4390.297.
- Key, R. M., A. Kozyr, C. L. Sabine, K. Lee, R. Wanninkhof, J. L. Bullister, R. A. Feely, F. J. Millero, C. Mordy, and T.-H. Peng (2004), A global ocean carbon climatology: Results from Global Data Analysis Project (GLODAP), *Global Biogeochem. Cycles*, 18, GB4031, doi:10.1029/2004GB002247.
- Key, R. M., et al. (2010), The CARINA data synthesis project: Introduction and overview, *Earth Syst. Sci. Data*, 2, 105–121.
- Kristjánsdóttir, G. B., D. W. Lea, A. E. Jennings, D. K. Pak, and C. Belanger (2007), New spatial Mg/Ca-temperature calibrations for three Arctic, benthic foraminifera and reconstruction of north Iceland shelf temperature for the past 4000 years, *Geochem. Geophys. Geosyst.*, 8, Q03P21, doi:10.1029/2006GC001425.
- Lea, D. W., T. A. Mashiotta, and H. J. Spero (1999), Controls on magnesium and strontium uptake in planktonic foraminifera determined by live culturing, *Geochim. Cosmochim. Acta*, 63, 2369–2379, doi:10.1016/S0016-7037(99)00197-0.
- Lear, C. H. (2007), Mg/Ca palaeothermometry: A new window into Cenozoic climate change, in *Deep-Time Perspectives on Climate Change: Marrying the Signal from Computer Models and Biological Proxies*, edited by M. Williams et al., pp. 313–322, Geol. Soc., London.
- Lear, C. H., H. Elderfield, and P. A. Wilson (2000), Cenozoic deep-sea temperatures and global ice volumes from Mg/Ca in benthic foraminiferal calcite, *Science*, 287, 269–272, doi:10.1126/science.287.5451.269.
- Lewis, E., and D. W. R. Wallace (1998), Program developed for CO₂ system calculations, Rep. ORNL/CDIAC-105, Carbon Dioxide Inf. Anal. Cent., Oak Ridge Natl. Lab., U.S. Dep. of Energy, Oak Ridge, Tenn., doi:10.2172/639712.
- Majoran, S., and S. Agrenius (1995), Preliminary observations on living *Krihe praetexta praetexta* (Sars, 1866), *Sarsicytheridea bradii* (Norman, 1865) and other marine ostracods in aquaria, *J. Micropaleontol.*, 14, 96, doi:10.1144/jm.14.2.96.
- Marchitto, T. M., W. B. Curry, and D. W. Oppo (2000), Zinc concentrations in benthic foraminifera reflect seawater chemistry, *Paleoceanography*, 15, 299–306, doi:10.1029/1999PA000420.
- Martin, P. A., D. W. Lea, Y. Rosenthal, N. J. Shackleton, M. Sarnthein, and T. Papenfuss (2002), Quaternary deep sea temperature histories derived from benthic foraminiferal Mg/Ca, *Earth Planet. Sci. Lett.*, 198, 193–209, doi:10.1016/S0012-821X(02)00472-7.
- McCorkle, D. C., P. A. Martin, D. W. Lea, and G. P. Klinkhammer (1995), Evidence of a dissolution effect on benthic foraminiferal shell chemistry: $\delta^{13}\text{C}$, Cd/Ca, Ba/Ca, and Sr/Ca results from the Ontong Java Plateau, *Paleoceanography*, 10, 699–714, doi:10.1029/95PA01427.
- Mehrbach, C., C. H. Culbertson, J. E. Hawley, and R. M. Pytkowicz (1973), Measurement of the apparent dissociation constants of carbonic acid in seawater at atmospheric pressure, *Limnol. Oceanogr.*, 18, 897–907, doi:10.4319/lo.1973.18.6.0897.
- Morse, J. W., and F. T. Mackenzie (1990), *Geochemistry of Sedimentary Carbonates*, Elsevier, New York.
- Oomori, T., H. Kaneshima, and Y. Maezato (1987), Distribution coefficient of Mg^{2+} ions between calcite and solution at 10–50°C, *Mar. Chem.*, 20, 327–336, doi:10.1016/0304-4203(87)90066-1.
- Poirier, R. K., T. M. Cronin, W. M. Briggs Jr., and R. Lockwood (2012), Central Arctic paleoceanography for the last 50 kyr based on ostracode faunal assemblages, *Mar. Micropaleontol.*, 88–89, 65–76, doi:10.1016/j.marmicro.2012.03.004.
- Rosenthal, Y., and G. P. Lohmann (2002), Accurate estimation of sea surface temperatures using dissolution-corrected calibrations for Mg/Ca paleothermometry, *Paleoceanography*, 17(3), 1044, doi:10.1029/2001PA000749.
- Rosenthal, Y., E. A. Boyle, and N. Slowey (1997), Temperature control on the incorporation of magnesium, strontium, fluorine, and cadmium into benthic foraminiferal shells from Little Bahama Bank: Prospects for thermocline paleoceanography, *Geochim. Cosmochim. Acta*, 61(17), 3633–3643, doi:10.1016/S0016-7037(97)00181-6.
- Rosenthal, Y., C. H. Lear, D. W. Oppo, and B. K. Linsley (2006), Temperature and carbonate ion effects on Mg/Ca and Sr/Ca ratios in benthic foraminifera: Aragonitic species *Hoeglundina elegans*, *Paleoceanography*, 21, PA1007, doi:10.1029/2005PA001158.
- Rosenthal, Y., A. Morley, C. Barras, M. E. Katz, F. Jorissen, G.-J. Reichert, D. W. Oppo, and B. K. Linsley (2011), Temperature calibration of Mg/Ca ratios in the intermediate water benthic foraminifer *Hyalinea balhica*, *Geochem. Geophys. Geosyst.*, 12, Q04003, doi:10.1029/2010GC003333.
- Rudels, B., E. P. Jones, U. Schauer, and P. Eriksson (2004), Atlantic sources of the Arctic Ocean surface and halocline waters, *Polar Res.*, 23(2), 181–208, doi:10.1111/j.1751-8369.2004.tb00007.x.
- Sabine, C. L., et al. (2004), The oceanic sink for anthropogenic CO₂, *Science*, 305, 367–371, doi:10.1126/science.1097403.
- Sarmiento, J. L., and N. Gruber (2006a), Carbon cycle, in *Ocean Biogeochemical Dynamics*, pp. 318–358, Princeton Univ. Press, Princeton, N. J.

- Sarmiento, J. L., and N. Gruber (2006b), Calcium carbonate cycle, in *Ocean Biogeochemical Dynamics*, pp. 359–391, Princeton Univ. Press, Princeton, N. J.
- Sosdian, S., and Y. Rosenthal (2009), Deep-sea temperature and ice volume changes across the Pliocene-Pleistocene climate transitions, *Science*, *325*, 306–310, doi:10.1126/science.1169938.
- Sosdian, S., and Y. Rosenthal (2010), Response to comment on “Deep-sea temperature and ice volume changes across the Pliocene-Pleistocene climate transitions,” *Science*, *328*, 1480, doi:10.1126/science.1186768.
- Stephens, C., J. I. Antonov, T. P. Boyer, M. E. Conkright, R. A. Locarnini, T. D. O’Brien, and H. E. Garcia (2002), *World Ocean Atlas 2001*, vol. 1, *Temperature*, NOAA Atlas NESDIS, vol. 49, NOAA, Silver Spring, Md.
- Tanhua, T., E. P. Jones, E. Jeansson, S. Jutterström, W. M. Smethie Jr., D. W. R. Wallace, and L. G. Anderson (2009), Ventilation of the Arctic Ocean: Mean ages and inventories of anthropogenic CO₂ and CFC-11, *J. Geophys. Res.*, *114*, C01002, doi:10.1029/2008JC004868.
- Vázquez-Rodríguez, M., F. Touratier, C. Lo Monaco, D. W. Waugh, X. A. Padin, R. G. J. Bellerby, C. Goyet, N. Metzl, A. F. Ríos, and F. F. Pérez (2009), Anthropogenic carbon distributions in the Atlantic Ocean: Data-based estimates from the Arctic to the Antarctic, *Biogeosciences*, *6*, 439–451, doi:10.5194/bg-6-439-2009.
- Yu, J., and W. S. Broecker (2010), Comment on “Deep-sea temperature and ice volume changes across the Pliocene-Pleistocene climate transitions,” *Science*, *328*, 1480, doi:10.1126/science.1186544.
- Yu, J., and H. Elderfield (2007), Benthic foraminiferal B/Ca ratios reflect deep water carbonate saturation state, *Earth Planet. Sci. Lett.*, *258*, 73–86, doi:10.1016/j.epsl.2007.03.025.
- Yu, J., and H. Elderfield (2008), Mg/Ca in the benthic foraminifera *Cibicides wuellerstorfi* and *Cibicides mundulus*: Temperature versus carbonate ion saturation, *Earth Planet. Sci. Lett.*, *276*, 129–139, doi:10.1016/j.epsl.2008.09.015.